

Self-Assembly of Octadecyltrichlorosilane on Graphene Oxide and the Tribological Performances of the Resultant Film

Junfei Ou,^{†,‡} Ying Wang,[§] Jinqing Wang,^{*,†} Sheng Liu,^{||} Zhangpeng Li,[†] and Shengrong Yang^{*,†}

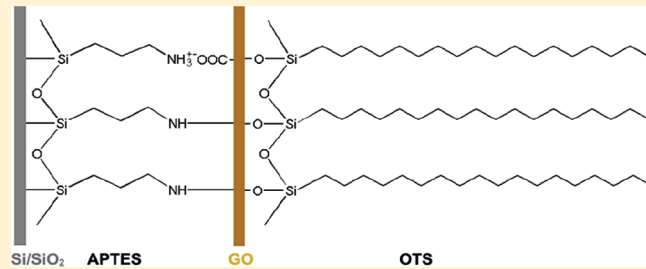
[†]State Key Laboratory of Solid Lubrication, Lanzhou Institute of Chemical Physics, Chinese Academy of Sciences, Lanzhou 730000, People's Republic of China

[‡]School of Materials Science and Engineering, Nanchang Hangkong University, Nanchang 330063, People's Republic of China

[§]Center for Low-Dimensional Materials, Micro/Nano Device and System, Changzhou University, Gehu Road 1, Changzhou 213164, People's Republic of China

^{||}The Technical Center of Zibo Entry-exit Inspection and Quarantine Bureau, Zibo 255031, People's Republic of China

ABSTRACT: Taking advantage of the condensation between Si—OH of the hydroxylated octadecyltrichlorosilane (OTS) and C—OH on graphene oxide (GO) surface, we grafted OTS onto the GO-based dual-layer film, which was composed of GO outerlayer and (3-aminopropyl)triethoxysilane (APTES) self-assembled underlayer, on a Si substrate. Thus, a hydrophobic trilayer film coded as APTES-GO-OTS was prepared successfully. To confirm the chemical composition, structure, and morphology of the trilayer film, various means including water contact angle measurement, attenuated total reflectance Fourier transform infrared (ATR-FTIR) spectrometry, X-ray photoelectron spectroscopy (XPS), and atomic force microscopy (AFM) were performed. Moreover, to investigate the tribological performances, the micro- and macrotribological experiments were conducted with AFM and a UMT tribometer. The results showed that the as-prepared trilayer film exhibited low adhesion and greatly reduced the friction force in both the micro- and macroscale. Therefore, such a trilayer film is suitable for an application in the lubrication and protection of nano/microelectromechanical systems (NEMS/MEMS).



1. INTRODUCTION

In recent years, chemical modification of graphene oxide (GO) sheets has become a popular research subject.^{1,2} This popularity is mainly promoted by three aspects. First, owing to reactive oxygen functional groups attached onto GO, it is very easy to perform such chemical modifications.³ Second, certain properties of GO, such as the conductivity and the dispersibility in nonpolar solvents, can be feasibly tuned by grafting with some molecules.^{3,4} Third, such modification is a promising route to achieve mass production of chemically modified graphene (CMG), which has found potential applications in many fields, such as polymer composites, energy-related materials, field-effect transistors, and lubricant coatings, etc.³

In our most recent study, taking advantage of the chemical reactions between epoxy/carboxyl and amine groups, GO sheets were covalently attached onto a self-assembled monolayer of (3-aminopropyl)triethoxysilane (APTES-SAM) covered Si substrate,⁵ resulting in the improved tribological behaviors. However, owing to the hydrophilicity of the GO surface, the adhesive force between the GO surface and an AFM tip was found to be in relatively high level. To reduce the high adhesive force, a post-treatment of thermal reduction was subsequently performed to decrease the content of the surface oxygenous groups. However, such a reduction procedure is relatively complicated and requires

an Ar atmosphere. In this article, we aimed at developing another easy way based on the chemical modification of GO to further improve the tribological performances of GO-based films.

As plenty of studies show, the hydroxyl groups on solid substrates (such as SiO₂/Al₂O₃) can induce the self-assembling of alkylsilanes (such as alkylchlorosilanes, alkylalkoxysilanes, and (alkylamino)silanes).⁶ Meanwhile, GO sheets are found to be attached with many hydroxyl groups. Therefore, it is rational to assume that an alkylsilane outerlayer can be formed on the GO surface. During the past decades, octadecyltrichlorosilane self-assembled monolayer (OTS-SAM) on Si substrate has been intensively studied as a lubricant coating for nano/microelectromechanical systems (NEMS/MEMS).^{7–14} It has been demonstrated that the OTS-SAM is hydrophobic and can reduce the adhesion/friction greatly. However, to the best of our knowledge, the attempt of assembling OTS on GO has not been performed by others. Herein, OTS molecules are selected as the grafting species and the detailed preparation procedures on GO surface are described as follows. First, an APTES-SAM with —NH₂ outer groups was covalently anchored onto the Si wafer

Received: January 20, 2011

Revised: April 22, 2011

Published: May 04, 2011

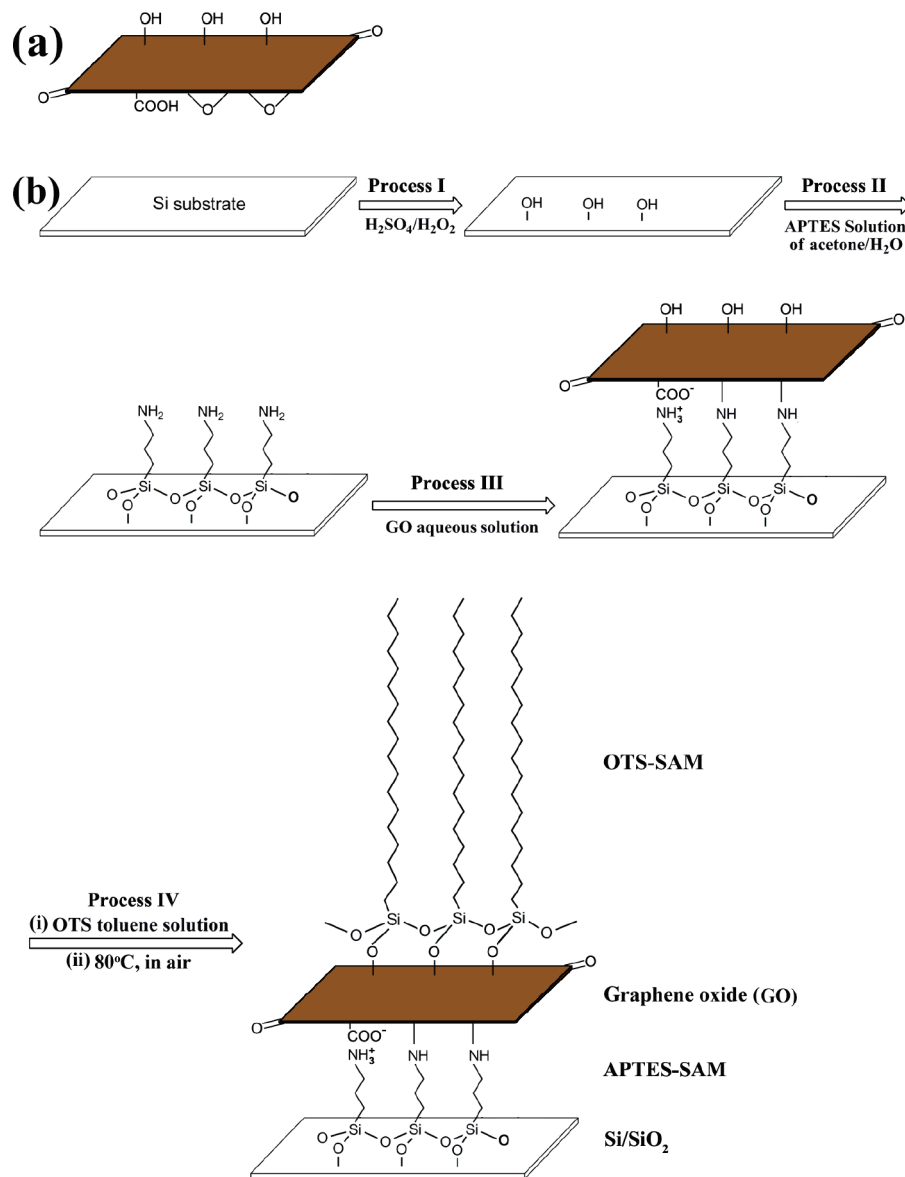


Figure 1

Figure 1. (a) Proposed chemical structure of GO. (b) Proposed schematic view for the construction of APTES-GO-OTS trilayer film on a Si wafer.

via Si—O—Si covalent bonding (Figure 1, process II). Then, GO sheets were chemo-grafted onto the APTES-SAM surface through certain chemical reactions (Figure 1, process III, the as-deposited sample was coded as APTES-GO). Finally, an OTS outerlayer was assembled onto the GO surface via C—O—Si bonding (Figure 1, process IV). The as-obtained trilayer film was coded as APTES-GO-OTS.

In brief, this work is a part of continuing efforts preparing self-assembled multilayer films with improved tribological behaviors, i.e., low friction coefficient and long antiwear life.^{5,12,15–22} As reported in our previous work, the dual layer film of APTES-GO is hydrophilic, possessing relatively low friction coefficient and good wear resistance.⁵ In this report, to increase the hydrophobicity of the film, an outerlayer of OTS-SAM is introduced, which is expected to reduce the friction and boost the antiwear life. Thus, a film with sandwiched microstructure and desirable composition was

constructed, aiming at developing thin-film lubricants suitable for NEMS/MEMS and other micro/nanodevices.

2. EXPERIMENTAL SECTION

2.1. Materials. Expandable graphite was obtained from Qingdao Hensen Graphite Co., Ltd. P-type polished single-crystal Si (111) wafers were purchased from GRINM Semiconductor Materials Co. (Beijing, China). (3-Aminopropyl)triethoxysilane (APTES, 99%) was purchased from Acros Organics. Octadecyltrichlorosilane (OTS, 90%) was provided by Sigma-Aldrich. Other chemicals were analytical grade and used as received. Ultra-pure water (>18 MΩ·cm) was used throughout the experiment.

2.2. Preparation of GO Colloid Solution. First, expandable graphite powder was heated at 1050 °C in air for 15 s. Then, 1 g of heat-treated expandable graphite was added to 23 mL of 98%

Table 1. WCA for the Silica Layer and the Modified Si Surfaces

test samples	Si/SiO ₂	APTES-SAM	APTES-GO	APTES-GO-OTS
WCA (deg)	~0	48.0 ± 1.6	40.8 ± 2.4	100.4 ± 3.6

H₂SO₄ in an ice bath with stirring, and 3 g of KMnO₄ was subsequently added slowly. The mixture was kept at 35 °C in a water bath for 30 min. Ultrapure water (46 mL) was gradually added, and the mixture was immersed in ice–water. After 20 min, the mixture was further treated with 140 mL of ultrapure water and 12 mL of 30% H₂O₂. The obtained mixture was first washed with ultrapure water until a pH level of 7 was reached and then was dialyzed under stirring until SO₄²⁻ anions could not be detected by the BaCl₂ solution (1 M). A diluted GO colloid solution with a concentration of 0.4 mg·mL⁻¹ was employed in the succeeding process.

2.3. Fabrication of Trilayer Film. Prior to assembly, Si wafers were cleaned and hydroxylated in a piranha solution (a mixture of 7:3 (v/v) 98% H₂SO₄ and 30% H₂O₂) at 90 °C for 30 min. [Caution: piranha solution is aggressive and explosive. Never mix piranha waste with solvents. Check the safety precautions before using it.] After being thoroughly rinsed with ultrapure water and blown dry with N₂, the Si wafers were immersed in a freshly prepared APTES solution (5 mM, the solvent is a mixture of acetone and water, with a volume ratio of 5:1) for 30 min. Then, the wafers were taken out and sonicated in ultrapure water, generating the desired APTES-SAM thereon. Subsequently, the APTES-SAM-covered Si substrate was kept in the prepared GO aqueous solution at 80 °C for 12 h and then ultrasonically cleaned in ultrapure water and blown dry with N₂. The obtained sample was coded as APTES-GO. At last, APTES-GO was immersed into an OTS solution (5 mM) of toluene for 12 h. After that, the sample was heated in air for 1 h at 80 °C to facilitate the anchoring of OTS molecules, followed by being ultrasonicated in toluene, acetone, and ultrapure water by turns. The as-prepared sample was coded as APTES-GO-OTS.

2.4. Characterization. Water contact angles (WCA) of different samples were determined using a DSA100 contact angle meter (Krüss). The reported data are average values of at least five repeat measurements for each sample (Table 1).

Attenuated total reflectance Fourier transform infrared (ATR-FTIR) spectra were recorded with an IFS 66 V/S FTIR spectrometer (Bruker) equipped with a Harrick Scientific horizontal reflection Ge-attenuated total reflection accessory (GATR, incidence angle 65°). The samples were placed in contact with the flat surface of a semispherical Ge crystal as the optical element. The spectrum was collected for 32 scans with a resolution of 4 cm⁻¹, and the background was collected using the accessory in the absence of the samples. To eliminate the effect of H₂O and CO₂, the pressure in the sample chamber and optical chamber was kept below 6.0 × 10⁻⁴ MPa.

X-ray photoelectron spectroscopy (XPS, PHI-5702, Physical Electronics) was performed using a monochromated Al Kα irradiation. The chamber pressure was about 3 × 10⁻⁸ Torr under testing condition. Peak deconvolution with Gaussian curves and quantification of elements were accomplished by Origin 7.0.

The surface morphologies of different samples were observed by a Nanoscope IIIa multimode atomic force microscope (AFM, Veeco) in tapping mode. The microtribological properties were measured using the same AFM in contact mode. Triangular

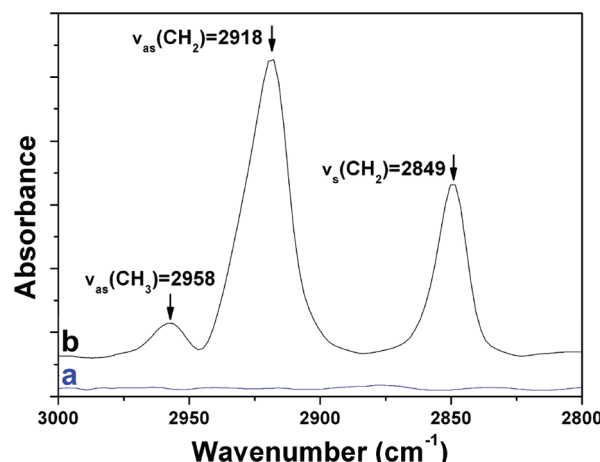


Figure 2. ATR-FTIR spectra of GO (a) and GO-OTS (b) on bare Si substrate.

Si₃N₄ cantilevers with a normal force constant of 2 N·m⁻¹ were employed for AFM measurements. As the lateral spring constant of the cantilevers and the lateral sensitivity of the optical detector were not measured, the absolute frictional force could not be obtained directly. The output voltages were directly used as the relative frictional force. The friction forces on various surfaces can be compared with one another when the same AFM tip is employed. To obtain the adhesive force between the AFM tip and the film surface, the force–distance curve was recorded on a CSPM 4000 AFM (Being Nano-Instrument). The pull-off force was considered as the adhesive force. Experiments were carried out under ambient conditions of 23 °C and relative humidity of 25%.

Macrotribological tests were run on a UMT-2MT tribometer (CETR) in a ball-on-plate contact configuration. Commercially availed steel balls (o.d. = 3 mm) were used as the stationary upper counterparts, while the lower Si wafers coated with different films were mounted onto the flat base and driven to reciprocally slide at a distance of 5 mm. The friction coefficient-versus-time curves were recorded automatically. At least three repeat measurements were performed for each frictional pair. The friction coefficient and antiwear life were measured at a relative error of ±10% and ±5%, respectively.

3. RESULTS AND DISCUSSION

3.1. Fabrication and Characterization of APTES-GO-OTS Film. The multistep assembly is facilitated by a popular material of GO, which is abundant with many attached oxygenous groups (such as hydroxyl, epoxy, and carboxyl) on its layer.^{23–25} Taking advantage of these polar groups, GO can be assembled onto certain substrates⁵ and served as an ideal host matrix for the accommodation of long silane alkyl chains.²⁶ The preparations of APTES-SAM and APTES-GO have already been performed in our previous studies.^{5,22} As experimental results indicate, GO can be chemo-grafted onto an APTES-SAM (with a thickness of 0.7 nm, which is in accordance with the reported value in literature²¹) surface successfully.⁵

The as-prepared APTES-GO is hydrophilic with many surface hydroxyl groups, which are expected to serve as the active points to induce the subsequent assembly of OTS molecules. To demonstrate the successful formation of OTS-SAM on GO, ATR-FTIR spectra of GO and GO-OTS on bare Si substrate

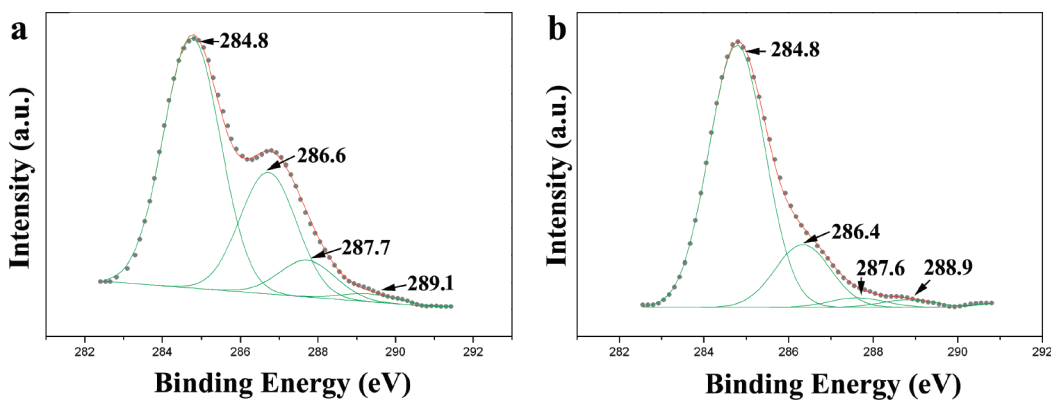


Figure 3. XPS spectra of C 1s for GO (a) and GO-OTS (b) on bare Si substrate.

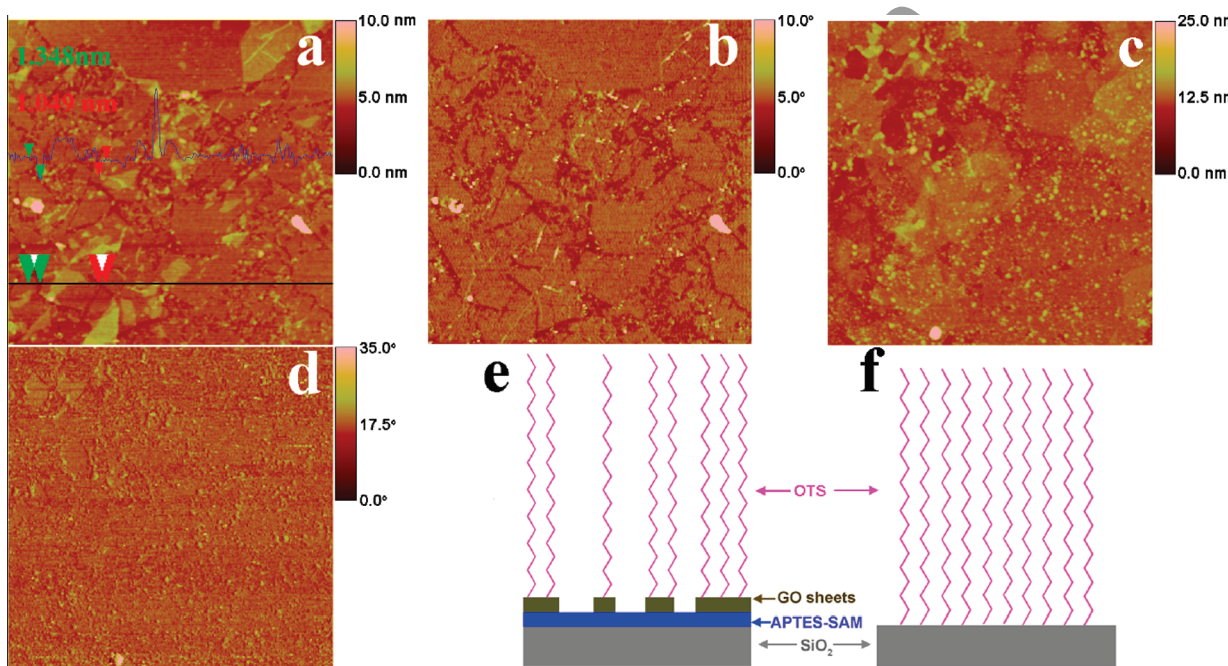


Figure 4. AFM images of APTES-GO (a) and APTES-GO-OTS (c) and phase maps of APTES-GO (b) and APTES-GO-OTS (d). The scanning area for (a) and (c) is $2.5\text{ }\mu\text{m} \times 2.5\text{ }\mu\text{m}$. The average roughness (R_a) and root-mean-square roughness (R_{ms}) for (a) and (c) are 0.476 and 1.258 nm and 1.061 and 1.666 nm, respectively. The thickness of GO sheets was estimated to be about 1.2 nm, which is in accordance with the literatures.^{42,43}

were recorded in the frequency range $3000\text{--}2800\text{ cm}^{-1}$ (Figure 2). After assembling of OTS molecules on GO, some new peaks located at 2958 , 2918 , and 2849 cm^{-1} emerge, which can be ascribed to the asymmetric methyl [$\nu_{as}(\text{CH}_3)$], asymmetric methylene [$\nu_{as}(\text{CH}_2)$], and symmetric methylene [$\nu_s(\text{CH}_2)$] vibrations, respectively (Figure 2b). As revealed by other researchers, tight packed chains in a well-ordered OTS monolayer exhibit a $\nu_{as}(\text{CH}_2)$ absorbance centered at approximately 2918 cm^{-1} .^{8,12} This reference value is the same with our result, so it is deduced that the alkyl chain of $-\text{C}_{18}\text{H}_{37}$ is in an ordered state. Furthermore, XPS spectra of GO and GO-OTS on bare Si substrate were also studied. As depicted in Figure 3a, the C 1s of GO can be deconvoluted into four Gaussian peaks corresponding to carbon atoms in different functional groups: C=C/C-C (nonoxygenated ring carbon, 284.8 eV), C-O (hydroxyl and epoxy, 286.6 eV), C=O (carbonyl, 287.1 eV), and O=C-OH (carboxyl, 289.1 eV).²⁷⁻²⁹ Upon the assembly of OTS thereon,

the C1s spectrum of APTES-GO-OTS (Figure 3b) confirms an obvious increase of nonoxygenated carbon related signals at 284.8 eV. According to the calculation of the integrated areas of the C 1s peaks, the content of C=C/C-C portion increased from 60.5% to 76.9%. Such increase is just attributed to the formation of OTS outlayer.

After chemo-grafting with OTS, the sample becomes hydrophobic with a WCA of 100.4° , which is much higher than that of APTES-GO (40.8°) but still lower than that of a compact OTS-SAM on the hydroxylated Si substrate (112°).³⁰ The relatively lower WCA value is supposed to be related to the incomplete coverage of OTS molecules. The AFM morphology in Figure 4a shows that the APTES-SAM modified Si substrate is discontinuously spread with irregular GO sheets. After the assembling of OTS, the surface becomes rougher and some narrow gaps as well as voids among GO sheets still exist (Figure 4c). Moreover, the phase maps were also given, indicating that the topological

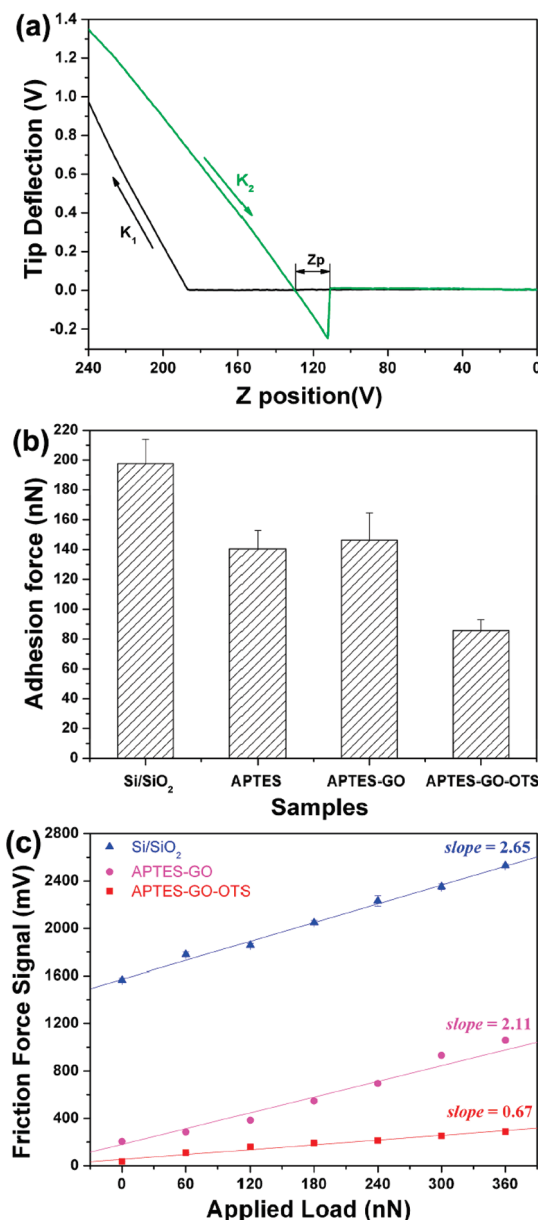


Figure 5. (a) Typical force–distance curve for Si/SiO₂. Adhesive force (b) and friction-versus-load curves (c) for different samples.

structure of the samples obtained from the topographic maps (Figure 4a,c) is in accordance with that obtained from the phase maps (Figure 4b,d). The structure and morphology of APTES-GO-OTS (Figure 4c) can be simulated by a simple model, as schematically illustrated in Figure 4e. It is rational that OTS cannot be grafted onto the gaps among GO sheets due to the mismatch between Si—OH (head groups of hydroxylated OTS) and —NH₂ (tail groups of APTES-SAM) groups. In other words, the Si wafer is not fully covered by OTS because of the discrete spreading of GO sheets. Consequently, the WCA of APTES-GO-OTS is lower than that of a compact OTS SAM on the Si substrate (Figure 4f).

3.2. Microtribological Behaviors. Stiction generated in NEMS/MEMS has been a major failure mode due to the large surface area-to-volume ratio.¹⁰ To estimate the antistiction behaviors of the synthesized films, the adhesive forces between

AFM tip and different surfaces are detected by an AFM. A typical force–distance curve of the Si/SiO₂ substrate was provided in Figure 5a. The pull-off force is reckoned as the adhesive force,^{31,32} which was given by

$$F = K_c \times Z_p \times (K_2/K_1)$$

where K_c is the force constant of the cantilever, K_2 and K_1 are the slopes of the corresponding lines as indicated in Figure 5a, Z_p is the vertical displacement of the piezo tube, i.e., the deflection of the cantilever. In Figure 5b, it was observed that strong adhesion was generated on the surfaces of hydrophilic Si/SiO₂ (197.7 nN), APTES-SAM (140.5 nN), and APTES-GO (146.2 nN). Upon the construction of APTES-GO-OTS, the surface became hydrophobic and the adhesive force decreased to 85.8 nN. This indicates that the OTS outerlayer exhibits low adhesion due to its hydrophobicity (100.4°). In other words, the adhesive force can be greatly reduced with increasing hydrophobicity of the surface. Such a phenomenon has also been observed in many researches and suggests that the modification of surface with long alkyl chain molecules can obviously lower the interfacial energy as well as the capillary force between the AFM tip and the surface.^{5,12,15–18,22,30,33–36}

The friction-versus-load curves for different surfaces were plotted in Figure 5c. It is apparent that the curves can be fitted by straight lines with nonzero intercepts. A similar result has been observed by Tsukruk, and the nonzero intercept is believed to be generated from the jump-to-contact instability caused by attractive forces during the approach of the tip to the sample surface.^{31,37} As the sample becomes hydrophobic, the adhesive force between AFM tip and sample surface decreases and such jump gets weak. For APTES-GO-OTS film, the smallest intercept was presented. To quantitatively evaluate the lubricity, a friction coefficient is generally necessary. However, it is hard to obtain the absolute value of the friction coefficient of the films in Figure 5c because the measured frictional force is expressed in raw voltage signal. To simplify this problem, relative friction coefficient (RFC), i.e., the slope of the fitted line, is introduced to compare with each other.^{5,19–22} As shown in Figure 5c, relative to Si/SiO₂, both APTES-GO and APTES-GO-OTS could reduce the friction force. Specifically, the lowest friction force (signal) for Si/SiO₂ is about 1560 mV, while the highest friction forces for APTES-GO and APTES-GO-OTS are about 1060 and 289 mV, respectively. Meanwhile, the trilayer of APTES-GO-OTS exhibited the lowest RCF. The excellent lubricity is attributed to the nature of the ordered OTS monolayer. On one hand, due to the hydrophobicity, the adhesive force as well as the interaction between AFM tip and OTS outerlayer is small. Such low interaction can reduce the dissipation of the accumulated energy during sliding and result in a low RCF.^{16,38,39} On the other hand, the ordered long alkyl chains of OTS with high packing energy would also decrease the energy dissipation and yield a low friction force.^{30,40,41}

3.3. Macro-Tribological Behaviors. The wear resistance capability is an important factor for lubricant films used in NEMS/MEMS. Figure 6 presents the curves of friction coefficient-versus-sliding time for different samples obtained by a ball-on-plate tribometer. Compared with APTES-SAM (Figure 6a), APTES-GO (Figure 6b) exhibited much lower friction coefficient (0.24) and longer antiwear life (~1520 s) at an applied load of 0.1 N. With increasing the applied load to 0.2 N, the antiwear life was shortened to ~180 s (Figure 6c). Once the OTS outerlayer was assembled, a much lower friction coefficient

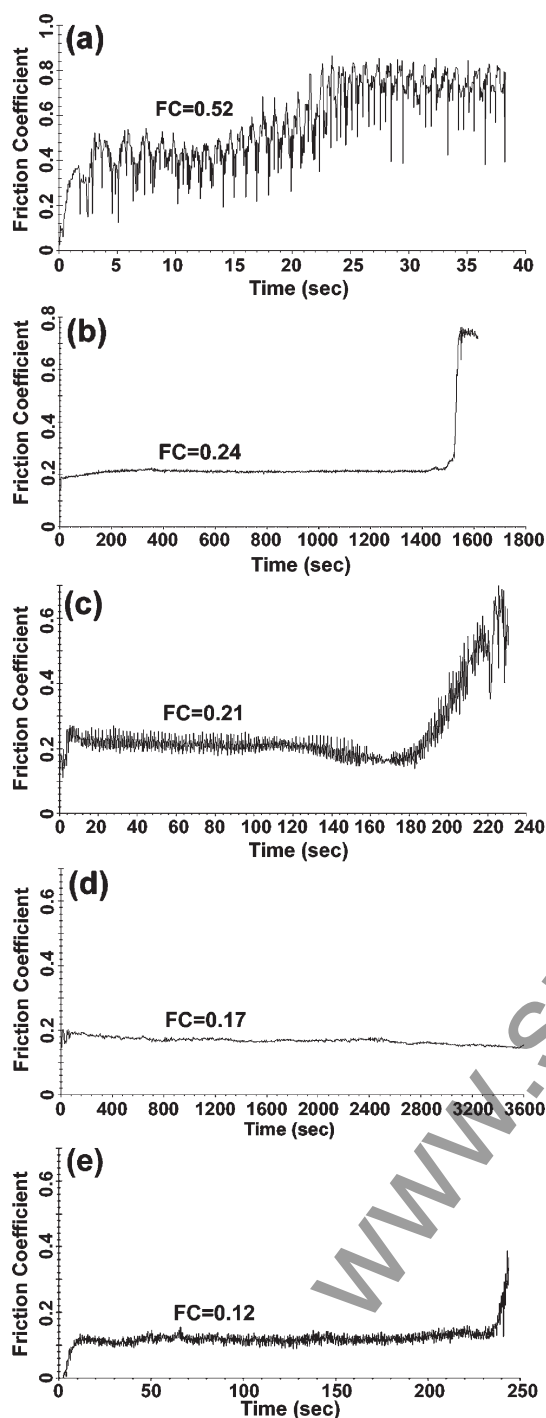


Figure 6. Variation in friction coefficient with time for various samples at different applied load and a sliding frequency of 1 Hz: (a) APTES-SAM, 0.1 N; (b) APTES-GO, 0.1 N; (c) APTES-GO, 0.2 N; (d) APTES-GO-OTS, 0.2 N; (e) APTES-C18, 0.2 N. The average friction coefficient (FC) was given above the corresponding curve.

(0.17) and a much longer antiwear life ($>3600\text{s}$) were achieved (Figure 6d). From these results, it can be concluded that the OTS outerlayer plays an important role in ameliorating the tribological behaviors. These improvements may be ascribed to the special structures of the OTS outlayer. Specifically, owing to the high flexibility and low surface energy of the OTS outerlayer, the friction coefficient for the trilayer decreases. Moreover, the OTS

monolayer possesses high elasticity and can endure larger stress, compression, and shear, without significant lateral displacement.³⁷ So, the wear-resistance of trilayer APTES-GO-OTS film is enhanced greatly.

In our previous work, the dual-layer film of APTES-C18 was also fabricated and the wear resistant performances were found to be good at an applied load of 0.1 N.¹⁵ While, in the present study, raising the applied load to 0.2 N, APTES-C18 dual-layer only exhibits an antiwear life $\sim 240\text{s}$ (Figure 6e), which is much shorter than that of APTES-GO-OTS. The obvious improvement in wear resistance is attributed to the composition difference between APTES-GO-OTS and APTES-C18. In other words, GO interlayer takes another main responsibility for the improved wear resistance. The enhancement mechanism might be attributed to the disordered structures of the GO sheets. Specifically, overlapped GO sheets (Figure 4a) tend to glide, just as the graphite lubricant, during the tribological tests.

From above discussions, it can be summarized that the as-prepared trilayer of APTES-GO-OTS possesses low friction and excellent wear-resistance due to the joint effect of GO and OTS molecules.

4. CONCLUSIONS

OTS molecules were chemo-grafted onto the surface of APTES-GO and correspondingly a hydrophobic trilayer film of APTES-GO-OTS was constructed successfully. The microstructures and tribological behaviors were investigated. Results indicate that the trilayer film exhibits much better tribological behaviors as compared with APTES-GO or APTES-C18, both of which were studied as lubricant films in NEMS/MEMS in our previous studies. So, this novel and feasible strategy is more suitable for construction of NEMS/MEMS lubricant coatings. Moreover, such modification is supposed to be applied in many other areas, such as to boost the hydrophobicity of graphene based biomaterials.

■ AUTHOR INFORMATION

Corresponding Author

*Tel: +86-931-4968076. Fax: +86-931-8277088. E-mail: jqwang@licp.ac.cn or sryang@licp.ac.cn.

■ ACKNOWLEDGMENT

We are grateful to the National Natural Science Foundation of China (Grant Nos. 20823008 and 51075384) and “Top Hundred Talents Program” of Chinese Academy of Sciences for financial support.

■ REFERENCES

- (1) Geim, A. K.; Novoselov, K. S. *Nat. Mater.* **2007**, *6*, 183–191.
- (2) Park, S.; Ruoff, R. S. *Nat. Nanotechnol.* **2009**, *4*, 217–224.
- (3) Dreyer, D. R.; Park, S.; Bielawski, C. W.; Ruoff, R. S. *Chem. Soc. Rev.* **2010**, *39*, 228–240.
- (4) Saovio, R.; Krabbenborg, S.; Naber, W. J. M.; Velders, A. H.; Reinoudt, D. N.; van der Wiel, W. G. *Chem.—Eur. J.* **2009**, *15*, 8235–8240.
- (5) Ou, J. F.; Wang, J. Q.; Liu, S.; Mu, B.; Ren, J. F.; Wang, H. G.; Yang, S. R. *Langmuir* **2010**, *26*, 15830–15836.
- (6) Ulman, A. *Chem. Rev.* **1996**, *96*, 1533–1554.
- (7) Bierbaum, K.; Grunze, M. *Langmuir* **1995**, *11*, 2143–2150.
- (8) Angst, D. L.; Simmons, G. W. *Langmuir* **1991**, *7*, 2236–2242.
- (9) GarciaParajo, M.; Longo, C.; Servat, J.; Gorostiza, P.; Sanz, F. *Langmuir* **1997**, *13*, 2333–2339.

- (10) Srinivasan, U.; Houston, M. R.; Howe, R. T.; Maboudian, R. *J. Microelectromech. Syst.* **1998**, *7*, 252–260.
- (11) Ashurst, W. R.; Yau, C.; Carraro, C.; Maboudian, R.; Dugger, M. T. *J. Microelectromech. Syst.* **2001**, *1*, 41–49.
- (12) Ren, S. L.; Yang, S. R.; Zhao, Y. P.; Zhou, J. F.; Xu, T.; Liu, W. M. *Tribol. Lett.* **2002**, *13*, 233–239.
- (13) Sung, I. H.; Yang, J. C.; Kim, D. E.; Shin, B. S. *Wear* **2003**, *255*, 808–818.
- (14) Khatri, O. P.; Devaprakasam, D.; Biswas, S. K. *Tribol. Lett.* **2005**, *20*, 235–246.
- (15) Ren, S. L.; Yang, S. R.; Zhao, Y. P. *Langmuir* **2003**, *19*, 2763–2767.
- (16) Ren, S. L.; Yang, S. R.; Wang, J. Q.; Liu, W. M.; Zhao, Y. P. *Chem. Mater.* **2004**, *16*, 428–434.
- (17) Ren, S. L.; Yang, S. R.; Zhao, Y. P. *Langmuir* **2004**, *20*, 3601–3605.
- (18) Ren, S. L.; Yang, S. R.; Zhao, Y. P. *Appl. Surf. Sci.* **2004**, *227*, 293–299.
- (19) Song, S. Y.; Ren, S. L.; Wang, J. Q.; Yang, S. R.; Zhang, J. Y. *Langmuir* **2006**, *22*, 6010–6015.
- (20) Song, S. Y.; Zhou, J. F.; Qu, M. N.; Yang, S. R.; Zhang, J. Y. *Langmuir* **2008**, *24*, 105–109.
- (21) Song, S. Y.; Chu, R. Q.; Zhou, J. F.; Yang, S. R.; Zhang, J. Y. *J. Phys. Chem. C* **2008**, *112*, 3805–3810.
- (22) Ou, J. F.; Wang, J. Q.; Liu, S.; Zhou, J. F.; Yang, S. R. *J. Phys. Chem. C* **2009**, *113*, 20429–20434.
- (23) Bourlinos, A. B.; Gournis, D.; Petridis, D.; Szabó, T.; Szeri, A.; Dékány, I. *Langmuir* **2003**, *19*, 6050–6055.
- (24) Dékány, I.; Krüger-Grasser, R.; Weiss, A. *Colloid Polym. Sci.* **1998**, *276*, 570–576.
- (25) Lerf, A.; He, H.; Forster, M.; Klinowski, J. *J. Phys. Chem. B* **1998**, *102*, 4477–4482.
- (26) Lee, B.; Chen, Y.; Duerr, F.; Mastrogiovanni, D.; Garfunkel, E.; Andrei, E. Y.; Podzorov, V. *Nano Lett.* **2010**, *10*, 2427–2432.
- (27) Yang, D. X.; Velamakanni, A.; Bozoklu, G.; Park, S.; Stoller, M.; Piner, R. D.; Stankovich, S.; Jung, I.; Field, D. A.; Ventrice, C. A., Jr.; Ruoff, R. S. *Carbon* **2009**, *47*, 145–152.
- (28) Stankovich, S.; Dikin, D. A.; Piner, R. D.; Kohlhaas, K. A.; Kleinhammes, A.; Jia, Y.; Wu, Y.; Nguyen, S. T.; Ruoff, R. S. *Carbon* **2007**, *45*, 1558–1565.
- (29) Tang, L. H.; Wang, Y.; Li, Y. M.; Feng, H. B.; Lu, J.; Li, J. H. *Adv. Funct. Mater.* **2009**, *19*, 2782–2789.
- (30) Xiao, X.; Hu, J.; Charych, D. H.; Salmeron, M. *Langmuir* **1996**, *12*, 235–237.
- (31) Tsukruk, V. V.; Bliznyuk, V. N. *Langmuir* **1998**, *14*, 446–455.
- (32) Xiao, X. D.; Qian, L. M. *Langmuir* **2000**, *16*, 8153–8158.
- (33) Khatri, O. P.; Biswas, S. K. *J. Phys. Chem. C* **2007**, *111*, 1696–2701.
- (34) Houston, J. E.; Doelling, C. M.; Vanderlick, T. K.; Hu, Y.; Scoles, G.; Wenzl, I.; Lee, T. R. *Langmuir* **2005**, *21*, 3926–3932.
- (35) Brewer, N. J.; Beaker, B. D.; Leggett, G. J. *Langmuir* **2001**, *17*, 1970–1974.
- (36) Tsukruk, V. V. *Adv. Mater.* **2001**, *13*, 95–108.
- (37) Bliznyuk, V. N.; Everson, M. P.; Tsukruk, V. V. *J. Tribol.-Trans. ASME* **1998**, *120*, 489–495.
- (38) Noy, A.; Frisbie, C. D.; Rozsnyai, L. F.; Wrighton, M. S.; Lieber, S. M. *J. Am. Chem. Soc.* **1995**, *117*, 7943–7951.
- (39) Frisbie, C. D.; Rozsnyai, L. F.; Noy, A.; Wrighton, M.; Lieber, C. M. *Science* **1994**, *265*, 2071–2074.
- (40) Mikulski, P. T.; Harrison, J. A. *J. Am. Chem. Soc.* **2001**, *123*, 6873–6881.
- (41) Houston, J. E.; Kim, H. I. *Acc. Chem. Res.* **2002**, *35*, 547–553.
- (42) Jung, I.; Dikin, D. A.; Piner, R. D.; Ruoff, R. S. *Nano Lett.* **2008**, *8*, 4283–4287.
- (43) Shen, J. F.; Hu, Y. Z.; Li, C.; Qin, C.; Shi, M.; Ye, M. X. *Langmuir* **2009**, *25*, 6122–6128.